Paper Type: Original Article

Evaluation of Protectivity of Aquifer Using Dar – Zarrouk Parameters in Ikot Ekpene Urban and its Environs

Emem Okon Ikpe[1],* (iD) **, Kufre Richard Ekanem[1]**

[1] Department of Science Technology, Akwa Ibom State Polytechnic, Ikot Osurua, Nigeria; emem.ikpe@akwaibompoly.edu.ng; ekanemkufre03@gmail.com.

Citation:

Abstract

The protective ability of hydrogeological units in the southern Nigerian region of Ikot Ekpene Urban and its environs was assessed in this work using the resistivity approach, namely Vertical Electrical Sounding (VES) and Electrical Resistivity Tomography (ERT) techniques. The lithological data from boreholes available indicates that the research region consists of three to four sandy strata (fine, coarse, and gravelly) with clay intercalations in some locations. With resistivity values ranging from 214.4 to 2839.0 Ωm, the third layer can be classified as gravelly sands in certain places or fine or coarse sands in others. Found between 9.0 and 86.6 meters below the surface, this layer is the main aquifer in the area. Using anisotropy coefficients, resistivity reflection, and longitudinal conductance, the aquifer protectivity was evaluated. Four zones are formed within the research area based on the protectivity grade. Regarding the proportion of exploitable aquifers, the zones are classified as poor (65%), weak (10%), moderate (20%), and good (5%). The surface topography affects the water table, and in the center of the region, a sinkhole develops. Utility pipes may be buried safely inside the stratum without fear of corrosion-induced damage because the heterogeneous topsoil has been shown to be non-corrosive. These results provide important new information for creating a successful groundwater and waste disposal plan in the area.

Keywords: Anisotropy coefficient, Longitudinal conductance, Resistivity reflection coefficient, Protectivity rating.

1 | Introduction

Water is a vital resource that is essential for the existence of life and is also the most abundant in the earth's system. It is present in many manifestations, namely surface water (streams, lakes, rivers, seas) and groundwater. Groundwater refers to the water that is located below the surface of the earth, specifically in rocks and soil.

It is kept underground in structures called aquifers. Surface water bodies have become contaminated, leading to a rising need for groundwater to accommodate the development of the world population [1–3]. Groundwater is an easily accessible substitute for water that can be used for domestic, public, and industrial purposes. It is particularly useful in areas where there are few surface water sources and often requires minimal treatment to make it safe to drink [4], [5]. Anthropogenic activities, such as inadequate waste disposal management, can negatively impact the quality of groundwater. These activities can result in the migration of harmful substances, known as leachates, from dumpsites into underground water sources.

Additionally, leakages from both surface and underground storage tanks, sewage from latrines, mining activities, and oil spillage can also contribute to the degradation of groundwater quality [6–8]. The aquifer system can be safeguarded by the layers of soil above it, known as the protective layers, which depend on their permeabilities, hydraulic conductivities, and thicknesses. Aquifer protectivity refers to the capacity of the layers above the aquifer to serve as natural barriers, effectively filtering surface-contaminated fluids that seep through [9], [10]. The protectivity of an aquifer is directly related to the thickness of the layers that provide protection and inversely related to the hydraulic conductivity of those layers [11–13]. The protectivity of the underlying hydrogeological units is primarily influenced by the permeability, grain size, porosity, and thickness of the protective layers [10], [14–16]. Permeable layers above, such as sand and gravel, have a high resistivity or low conductivity and a high hydraulic conductivity. As a result, they allow surface contaminants to infiltrate into the aquifer system easily. The protection of aquifers is improved with this approach [10], [17], [18].

The protectivity of an aquifer can be assessed by analyzing secondary geoelectric indices generated from the interpretation of resistivity-sounding data. The overall conductivity of the protective layers in the longitudinal direction is directly related to the ability of the aquifer to defend itself [9], [13]. Overburden layers with a total longitudinal unit conductance greater than one are linked to impervious materials, which provide good or excellent protection. Conversely, values below 0.1 are typically associated with previous overburden layers, which offer weak or poor protection to the underlying aquifer systems. A permeable layer with low resistivity, such as clay or shale, that is located above an impermeable layer with high resistivity, such as sands and gravels, will result in a negative resistivity Reflection Coefficient (RC). This characteristic can also be utilized to evaluate the effectiveness of aquifer systems in providing protection. RCs with negative values indicate high levels of protectivity, whereas positive values indicate lower levels of protectivity [15], [17].

Furthermore, it is worth noting that the resistivity of earth materials can exhibit variation in different directions, which is known as resistivity anisotropy [19]. In this scenario, the coefficient of resistivity anisotropy is higher than one. Georesistivity anisotropy can arise from the alternating layers of sand and clay [20] and can, therefore, indicate the extent of surface water penetration into the subsurface [15]. The protectivity of hydrogeological units in Ikot Ekpene urban and its surrounding areas in southern Nigeria was evaluated using these three characteristics. The corrosiveness of the outermost layer was also evaluated based on the resistivity of the layer, which is a fundamental geoelectric indicator.

The rapid increase in population and urbanization over the past decade has led to a significant rise in the problem of water shortage in the Ikot Ekpene metropolitan area and its surrounding areas. An expedient measure to address the issue of water scarcity has been a surge in the investigation of underground water sources. A significant amount of solid garbage, consisting of various types such as household waste, vegetable waste, paper waste, metal scraps, chemical-containing cans, plastic containers, old fabric, vehicle tires, scalpels, and human waste, persistently pollutes the streets of Ikot Ekpene Urban [21]. Certain types of garbage are classified as hazardous and have the potential to create significant health problems if they contaminate the residential water supply. Hence, it is necessary to evaluate the ability of the hydrogeological units in the area to preserve the groundwater and manage waste disposal effectively. This assessment will help establish a plan that ensures the safety of the current and future populations.

Geology and location of the study area

This study was conducted in the urban area of Ikot Ekpene and its surrounding areas. Ikot Ekpene, sometimes referred to as the Raffia City is located in the northwestern region of Akwa Ibom State in southern Nigeria (*Fig. 1*). It is positioned between latitudes 5.072°–5.140° N and longitudes 7.390°–7.458° E.
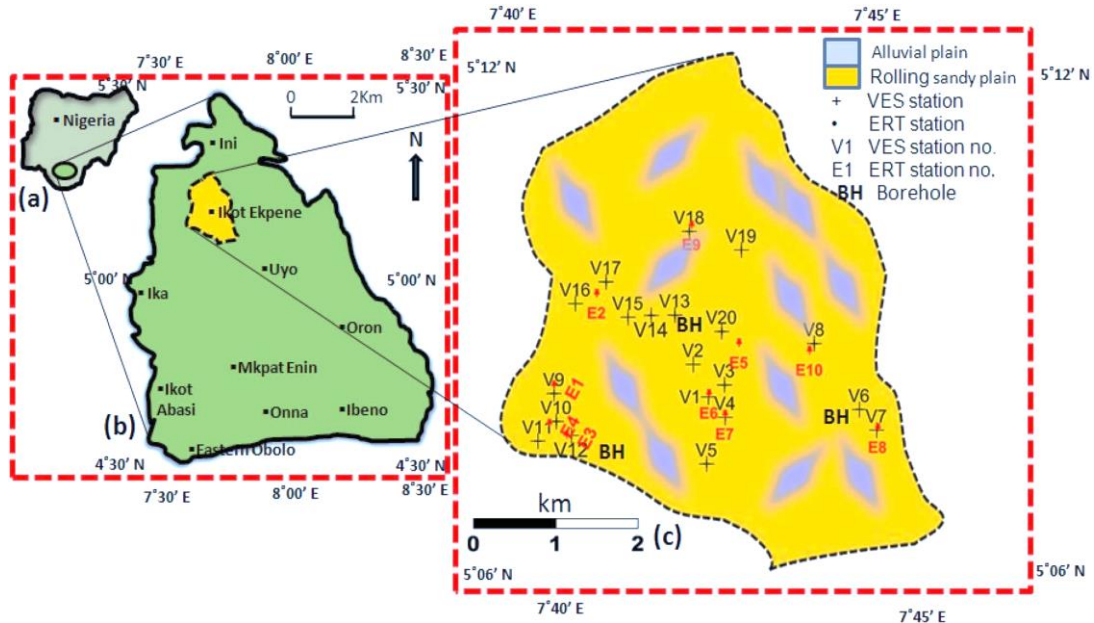

Fig. 1. Map of a Nigeria showing Akwa Ibom State in southern Nigeria, b Akwa Ibom State showing the study area, and c study area showings its geology and sounding stations.

It covers an approximate area of 25 square kilometres. The region exhibits a gently rolling terrain, with elevated areas in the north and a gradual descent towards the southwest. The highest point above sea level in the area is approximately 102 meters in the northern region. In comparison, the lowest point is around 54 meters in the southern region (*Fig. 2*). The arrows depicted in *Fig. 2* illustrate the trajectory of surface water (rain) movement, predominantly directed towards the ravine situated in the southwestern region of the land. The placement of the dumpsites in the ravine may have been required due to the direction of surface water flow, as depicted in *Fig. 2*. The region experiences extensive drainage due to the presence of inland coastal water. The vegetation in the studied area exhibits characteristics typical of a rainforest ecosystem. The area experiences a high average relative humidity of 83% and receives a significant amount of precipitation, with an annual average of 250 mm [22].
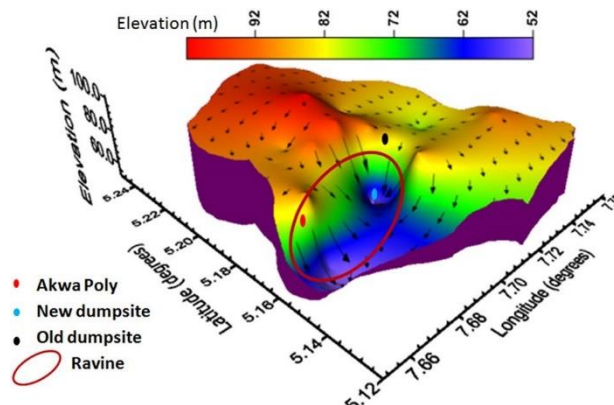
Fig. 2. Topography map of study area showing the direction of surface water flow.

Ikot Ekpene is located in an area with a humid tropical climate. This climate is characterized by two different seasons: the wet or rainy season, which occurs from March to October, and the dry season, which occurs from November to April [22]. Geographically, Ikot Ekpene is situated in the Niger Delta region, which is positioned right on the Gulf of Guinea on the Atlantic Ocean in Southern Nigeria. The predominant geological composition of the area consists of Coastal Plain Sands (CPS), specifically belonging to the Benin

Formation [23]. The Formation at the highest point of the Niger Delta consists of sands and gravels that are not well sorted, with a range of grain sizes from fine to coarse [23], [24]. The Agbada Formation, located in the Niger Delta region, is a significant hydrocarbon-bearing unit that underlies the Benin Formation [24], [25]. The primary hydrogeological units in the research region are the CPS, which are characterized by the presence of clay and sandy clay in certain localities [26]. At various areas in the area, a multi-aquifer system is formed by the accumulation of alternating sand and clay layers [2], [27], [28]. The Agbada Formation is situated below the Akata Formation, which forms the base of the Delta [24], [25]. The schematic diagram in *Fig. 3* illustrates the broad stratigraphy of the Niger Delta, which includes the research region.
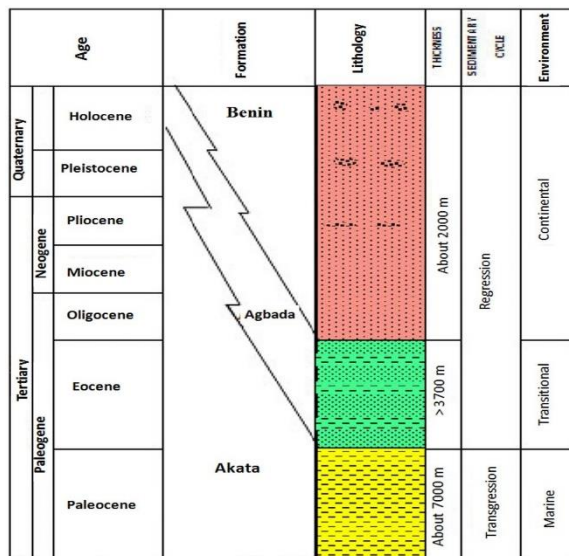

**Fig. 3. A schematic diagram showing the general Stratigraphy of the Niger Delta,
where the study area is located [29].**

2 | Materials and Method

2.1 | Resistivity Survey

This study utilized two resistivity measuring approaches to sample the resistivity distribution in the subsurface. The IGIS signal enhancement resistivity meter SSP-MP-ATS and its accessories were employed for this purpose. The two techniques used are Vertical Electrical Sounding (VES) and Electric Resistivity Tomography (ERT). Both methods involve the placement of two electrodes, referred to as the current electrodes (A and B), on the surface of the earth to introduce an electric current into the subsurface. Additionally, two corresponding potential electrodes (M and N) are positioned on the surface to measure the resulting potential difference. The resistivity meter was linked to all four electrodes arranged in a line. The meter's output LED display indicated the ratio of the potential difference to current, which represents the apparent resistance of the earth layers that the electric current passed through. The extent of penetration is directly proportional to the increase in the distance between the current electrodes [2], [3], [16]. The VES approach employed the Schlumberger electrode configuration, whereas the ERT technique utilized the Wenner electrode configuration. The Schlumberger electrode arrangement entails incrementally increasing the distance between the current electrodes AB and, on occasion, the distance between the potential electrodes MN around the central part of the array in order to collect samples from deeper layers. The study found that the distance AB varied between 2 and 400 meters, whereas the distance MN varied between 0.5 and 20 meters. The electrode spacing in all the occupied sounding locations was set to ensure that AB is more than or equal to 5 MN, as per the assumption of potential gradient [30], [31]. The Wenner arrangement, on the other hand, requires the employment of a consistent distance between electrodes, which can be progressively raised to sample deeper layers at regular intervals. In the study for the ERT scenario, the initial electrode spacing was kept constant at 5 m. The spacing was then increased in increments of 5 m until a total spread length of 105 m was reached, following the methodology described in [3].

The purpose of this investigation was to examine any horizontal differences in the electrical resistivity of the shallow layers in order to compare them with the VES results for the corresponding shallow layers. A total of 20 VESs and 10 ERTs were conducted in the study region. The spatial arrangement of these sounding stations, which was limited by the road network and physical infrastructure, is illustrated in *Fig. 1*. Several soundings were conducted near existing boreholes that had lithological data available in the vicinity. This was done to assist in the computer interpretation of the gathered data. The lithological data provided limitations on the identification of the lithological and hydrogeological units in the area. *Fig. 4* displays the arrangement of the field for collecting data using the VES approach in the research region.

Fig. 4. Field set up for data acquisition using the VES technique. The main measuring equipment was the resistivity meter with the electrodes, cables and other accessories.

2.2|Resistivity Data Analysis

The apparent resistivity for each approach used in this investigation was calculated for each station by multiplying the observed resistance with the associated geometric parameters. The geometric factors KS and KW for the Schlumberger and Wenner arrays are determined by Eq. (1) and Eq. (2), respectively.

$$K_S = \pi \cdot \left[\frac{(AB/2)^2 - (MN/2)^2}{MN} \right].$$ (1)

$$K_W = 2\pi a,$$ (2)

where AB, MN, and a are current electrode separation, potential electrode separation and Wenner constant electrode separations, respectively.

The VES data involved plotting the apparent resistivity values for each sounding station against half of the current electrode separation (AB/2) on a log-log scale, resulting in the creation of sounding curves. The curves were later smoothed to eliminate noisy signatures, which could potentially cause errors in the computer modeling phase of data interpretation [2], [16], [17]. This was accomplished by calculating the mean of the two apparent resistivity values at crossover distances. Any outliers were removed while ensuring that the major trend of the curve was preserved. The traditional curve matching technique was employed to analyze each of the smoothed field curves in order to get the initial resistivities and thicknesses of the layers [32]. The initial layer indices were utilized as inputs in the computer-aided quantitative interpretation. In this investigation, the interpretation was conducted using a One-Dimensional (1D) least square forward modeling software tool called WINRESIST [33]. The software utilizes the input data to create a theoretical model. Subsequently, it establishes a correlation between the model and the observed field data, resulting in the final 1D resistivity model curves. The adequacy of the fit is quantified using the Root-Mean-Square Error (RMSE)

[34], which varied between 2.3% and 3.1%. *Fig. 5.a* displays a screenshot of the WINRESIST window during the calculation of the theoretical model, while *Fig. 5.b* shows the matching resist graph display. This inversion method was constrained using data from the three existing boreholes in the area. *Fig. 7* displays the final model curves for VES 4, 7, 12, and 20, along with the accompanying drill lithological data. The geoelectric indices obtained from these final model curves are the genuine resistivity, thickness, and depth of each layer, respectively.
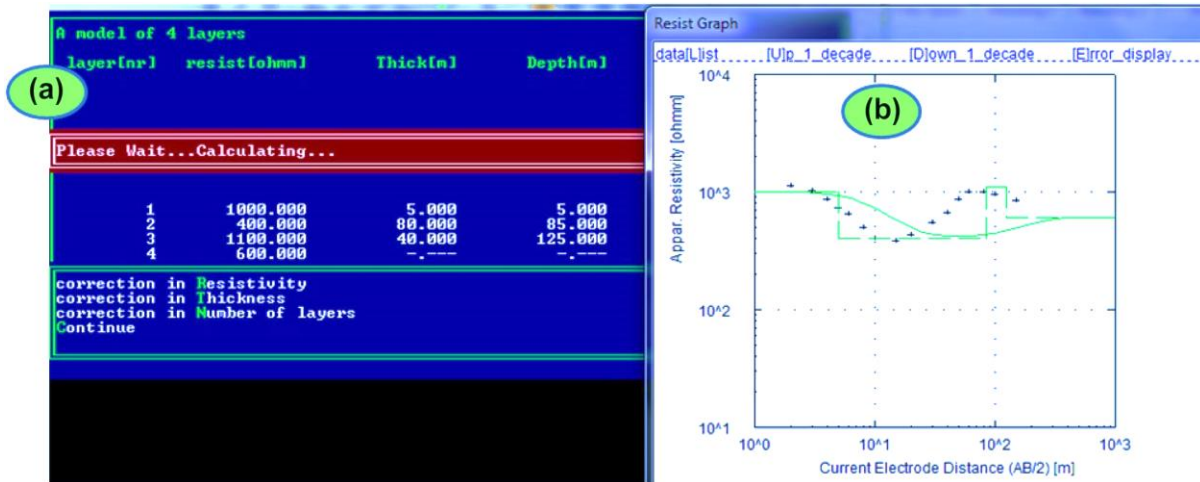

Fig. 5. A snapshot of the WINRESIST window during the data analysis; a) command window where calculation of the theoretical model is ongoing using the initial layer parameters as inputs, b) display window showing the resist graph.

In this investigation, the ERT data was inverted in Two-Dimensions (2D) using a computer modeling software tool called RES2DINV [35–37]. The RES2DINV software utilizes the supplied field data to generate a theoretical model and then compares it to the actual field data. In the instance of the VES interpretation, the goodness of fit is quantified using the RMSE, which varied between 9.7% and 45.1%. *Fig. 6* displays a momentary view of the RES2DINV window while conducting the 2D data inversion.
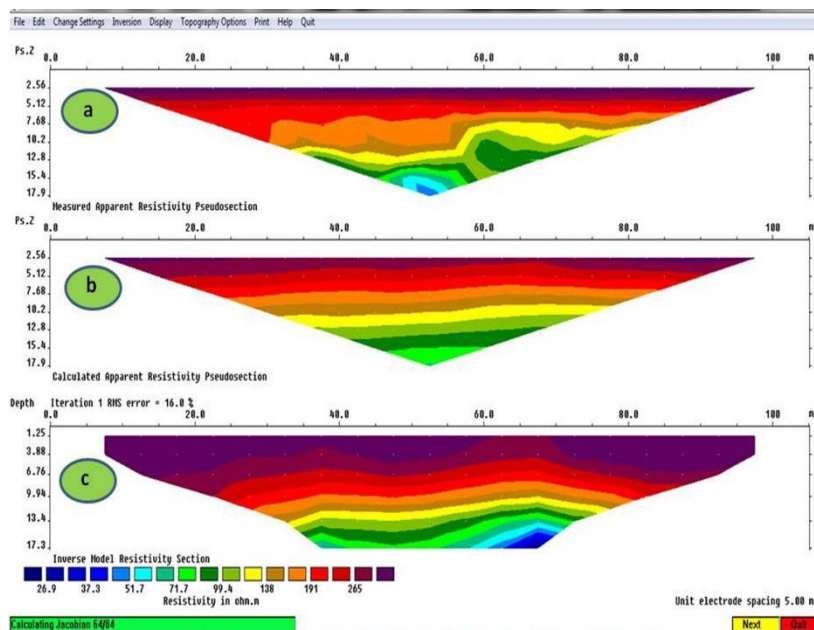
Fig. 6. A snapshot of the RES2DINV window during the 2D data inversion; a) measured apparent resistivity pseudosection, b) Calculated theoretical model resistivity pseudosection, c) Inverse model resistivity pseudosection, which is the true resistivity variation of the subsurface.

In *Fig. 6*, a) the uppermost panel, displays the measured apparent resistivity pseudosection, b) the middle panel, presents the calculated theoretical model resistivity pseudosection, and c) the lower panel, exhibits the inverse

model resistivity pseudosection, which represents the actual resistivity variation of the subsurface. The 2D modelling yielded the accurate resistivity distribution of the shallow subsurface that was penetrated by the current, resulting in the final picture sections. *Fig. 7* displays examples of these picture sections for ERTs 3, 5, 7, and 8, with the final VES model curves (VESs 4, 7, 12, and 20), facilitating straightforward comparison and linkage with the drill lithological log. By comparing the lithological data obtained from the boreholes near VESs 4, 7, 12, and 20 with the VES curves depicted in *Fig. 7*, it is evident that the primary aquifer in the region is located in the third layer. Nevertheless, the aquifer depths predicted from the VES curves do not completely align with the depths determined from the borehole lithological log. This discrepancy can occur because geological sections may not align precisely with geo-electrical sections [38]. The findings of the ERT interpretations exhibit a reasonably strong correlation with the borehole lithological log.
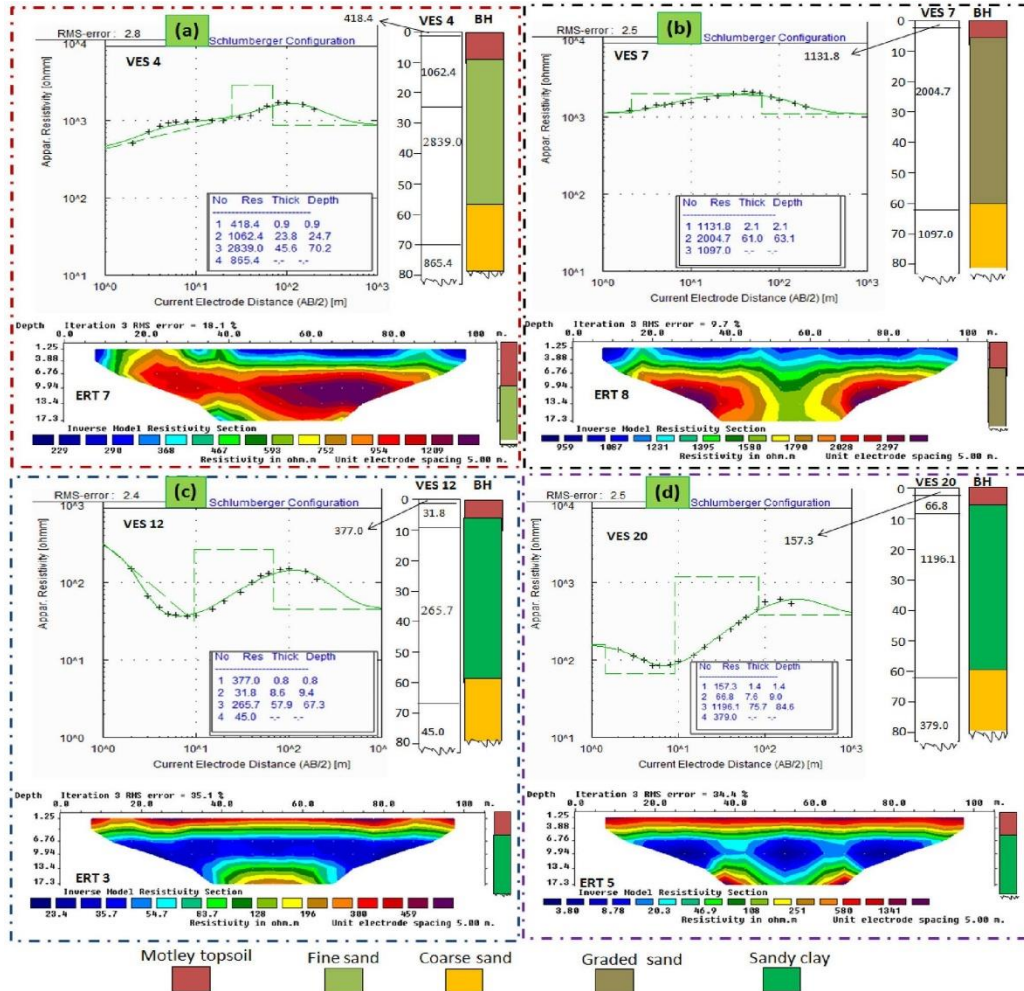
Fig. 7. Sample interpreted VES curves and corresponding ERT sections at; a. Utu Ikpe, b. Utu-Uyo Road, c. AKWAPOLY, d. Library Avenue. The results of both VES and ERT interpretations correlate fairly well with the borehole lithological log.

2.2.1|Assessment of protectivity of hydrogeological units

The level of protection provided by a specific hydrogeological unit is contingent upon the characteristics of the geomaterials that lie above it. In this context, protectivity refers to the capacity of the upper layers, also known as the protecting layers, to slow down and purify surface fluid that is seeping through [9], [17]. The protectivity of the underlying hydrogeological units is influenced by several critical parameters, including permeability, grain size, porosity, and thickness of the protective layers [10], [14–17]. The presence of thick and impermeable layers with poor hydraulic conductivity will slow down the rate at which water enters the subsurface, hence increasing the protective nature of the aquifer system [10], [17].

The protectivity of hydrogeological units can be evaluated by utilizing both the thickness of the overburden layer and its resistivity [11]. The longitudinal conductance can be calculated using these two main geoelectric indices. The aquifer protectivity is directly proportional to the longitudinal conductance [11–13]. The longitudinal conductance S_i of a layer of thickness h and resistivity ρ is mathematically defined as

$$S_i = \frac{h_i}{\rho_i}. \tag{3}$$

The formula for the total longitudinal conductance S of a stacked n layers is as follows:

$$S_L = \sum_i^n \frac{h_i}{\rho_i}. \tag{4}$$

The resistivity RC and anisotropy coefficient (λ) are two additional secondary geoelectric indices that can be utilized to evaluate the protective nature of hydrogeological units [15], [17]. The resistivity RC provides data on the change in electrical resistivity between the layers of the ground. The computation can be performed using Eq. (5).

$$RC = \frac{\rho_2 - \rho_1}{\rho_1 + \rho_2}, \tag{5}$$

where ρ_1 and ρ_2 are the resistivity of the top and the underlying layers, respectively.

The anisotropy coefficient is defined by the transverse resistivity and longitudinal resistivity, as given by Eq. (6).

$$\lambda = \sqrt{\frac{\rho_v}{\rho_h}}. \tag{6}$$

The transverse resistivity, ρ_v, and the longitudinal resistivity, ρh, are provided in Eq. (7) and Eq. (8) correspondingly.

$$\rho_v = \frac{\sum_i^n h_i \rho_i}{\sum_i^n h_i}. \tag{7}$$

$$\rho_h = \frac{\sum_i^n h_i}{\sum_i^n \frac{h_i}{\rho_i}}. \tag{8}$$

In the context of a stack of earth layers, the current flow is perpendicular to the layers when considering transverse or vertical resistivity (ρ_v). On the other hand, for longitudinal or horizontal resistivity, the current flow is parallel to the layers, as shown in *Fig. 8*.

Gravels and sands, which are permeable materials, have low longitudinal conductance or high resistivity. On the other hand, clay and shale, which are impervious materials, have high longitudinal conductance or low resistivity [10], [18]. Materials with a longitudinal conductance of less than 0.1 are typically linked to inadequate aquifer protectivity, whereas values of longitudinal conductance larger than 1 are associated with strong aquifer protectivity [11–13].
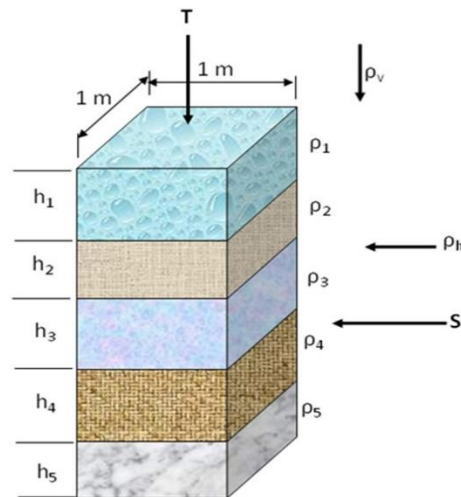
Fig. 8. 3D layered earth model used to derive the anisotropy coefficient and Dar zarrouk parameters [39].

The resistivity RC of any pair of earth layers can exhibit positive or negative values, contingent upon the resistivities of the respective layers. When the resistivity of the top layer is higher than the resistivity of the lower layer, the RC value is negative. Conversely, when the resistivity of the lower layer is higher than the resistivity of the top layer, the RC value is positive. As a result, RC values will be negative when a layer with low resistivity, such as clay or shale, is found beneath a layer with high resistivity, such as sandy or gravelly material that is permeable. Therefore, negative RC values indicate a pattern of impermeable-permeable layers of soil, which might lead to a reduced rate of water penetration, thereby safeguarding any underlying hydrogeological units. Georesistivity anisotropy may arise from a narrow series of sand-clay intercalation [15], [20]. When the anisotropy coefficient of the overburden layers is equal to one, the aquifer system may lack protection [15]. This study utilized three secondary geoelectric indices to evaluate the protective nature of the hydrogeological units in the designated study region.

3 | Results and Discussion

3.1 | VES and ERT Results

The interpretation of the VES data reveals that the research area consists of 3-4 geoelectric layers within the maximum current electrode spread used. The findings are succinctly presented in *Table 1*. The initial stratum, identified as the diverse surface soil, exhibits resistivity values ranging from 157.3 to 1278.2 Ωm and has a thickness ranging from 0.6 to 19.2 m. This layer spans the entirety of the research region. The observed substantial fluctuation in resistivity in this layer may be attributed to the artificial composition of the layer and the ongoing bioturbating activities inside it [40]. The analysis discovered a second layer at a depth of 0.6–19.2 m with a resistivity range of 31.8–2648.10 Ωm. This layer was characterized as sandy clay in certain spots and fine/graded sand in other regions. The observed fluctuation in resistivity in this layer can be attributed to the varying particle sizes of the geomaterials present. These grain sizes are representative of the CPS found in the Niger Delta [23], [24]. In the studied region, the third geoelectric layer is found at a depth of 9.0–86.6 m and has a resistivity range of 214.4–2839.0 Ωm. This layer represents the hydrogeological units (aquifer) that are economically important for groundwater extraction in the area. It consists mostly of fine/coarse and gravelly sands, as indicated by the borehole lithological log. The aquifer layer at specific sites (VESs 1, 2, 4, 5, 8, 9, 13, 15, and 19) has high resistivity values over 1500 Ωm. This phenomenon can be attributed to the presence of gravelly sand, which is confirmed by the borehole lithological log. This phenomenon can be attributed to the fact that the resistivity of the second layer is comparatively lower than that of the aquifer layer at certain sites, as seen in *Table 1*.

Table 1. Failure mechanisms of BOP annular using failure mode and effect analysis.

VES no	Location	Longitude (∘)	Latitude (∘)	Elevation (m)	No. of layers	Layer resistivity (Ωm)				Layer thickness (m)			Layer depth (m)			Curve Typ
						$\overline{\rho_1}$	ρ_2	ρ_3	ρ_4	$\overline{h_1}$	h_2	h_3	$\overline{d_1}$	d_2	d_3	
1	Dumpsite I-utu ikpe	7.7038	5.1644	62.0	4	1190.2	248.6	1750.8	418.7	2.6	8.5	49.2	2.6	11.1	60.3	HK
2	Dumpsite 2-utu ikpe	7.7031	5.1656	54.0	3	1278.2	639.4	1621.6		5.6	56.7	-	5.6	62.3		H
3	Utu ikpe near prison	7.7053	5.1631	75.0	3	430.7	2283.3	851.2		1.1	60.4	-	1.1	61.5		K
4	Utu ikpe near palace	7.7078	5.1598	88.0	4	418.4	1062.4	2839.0	865.4	0.9	23.8	45.6	0.9	24.7	70.3	AK
5	Abiakpo edem idim	7.7033	5.1491	72.0	4	1028.8	339.2	2129.4	760.3	0.6	10.4	54.0	0.6	11.0	65.0	HK
6	Ibiakpan nto akan	7.7400	5.1615	86.0	3	193.5	831.7	1341.6		1.6	64.4	-	1.6	66.0		A
7	Utu-uyo road	7.7442	5.1568	91.0	3	1131.8	2004.7	1097.0		2.1	61.0	-	2.1	63.1		K
8	Ikpon road	7.7292	5.1767	78.0	4	590.7	149.2	2478.6	827.9	1.3	11.1	61.4	1.3	12.4	73.8	HK
9	Abiakpo ntak inyang	7.6667	5.1652	89.0	3	487.8	1021.5	2632.2		2.1	53.5	-	2.1	55.6		A
10	Akwa poly PI	7.6672	5.1588	57.0	3	334.0	89.6	214.4		19.2	67.4	-	19.2	86.6		H
11	Akwa poly P2	7.6706	5.1539	54.0	4	590.8	72.1	722.9	83.3	5.5	16.7	45.2	5.5	22.2	67.4	HK
12	Akwa poly P3	7.6708	5.1556	55.0	4	377.0	31.8	265.7	45.0	0.8	8.6	57.9	0.8	9.4	67.3	HK
13	Ikot ekpene housing, ifuho	7.6914	5.1832	97.0	3	441.5	1848.3	2405.8		3.6	63.4	-	3.6	67.0		A
14	Ifuho	7.6900	5.1831	93.0	3	473.4	79.4	445.7		2.0	52.3	-	2.0	54.3		H
15	Ifuho	7.6844	5.1827	93.0	3	170.7	925.1	1959.4		1.7	68.1	-	1.7	69.8		A
16	Ibong ikot akan	7.6775	5.1866	88.0	3	228.5	2111.6	434.5		6.1	49.3	-	6.1	55.4		K
17	Ibong road	7.6792	5.1908	88.0	4	431.9	40.6	375.5	75.6	1.4	14.6	47.5	1.4	16.0	63.5	HK
18	Umuahia road	7.6992	5.2024	102.0	4	224.4	59.1	1264.5	324.9	2.1	8.4	59.9	2.1	10.5	70.4	HK
19	Ikono road	7.7117	5.1981	85.0	3	207.4	2648.1	1506.3		4.5	80.9	-	4.5	85.4		K
20	Progress road	7.7069	5.1794	90.0	4	157.3	66.8	1196.1	379.0	1.4	7.6	75.7	1.4	9.0	84.7	HK
	Minimum			54.0		157.3	31.8	214.4	45.0	0.6	7.6	45.2	0.6	9.0	60.3	
	Maximum			102.0		1278.2	2648.1	2839.0	865.4	19.2	80.9	75.7	19.2	86.6	84.7	
	Mean			79.9		519.4	827.6	1376.6	420.0	3.3	39.4	55.2	3.5	42.7	69.2	

The aquifers are often unconfined, as shown by the absence of impermeable confining layers observed in the VES results. This finding aligns with the geological information obtained from the boreholes. The stacked ID pictures in *Fig. 9* display the spatial distribution of resistivity for the first three layers found in the research region.
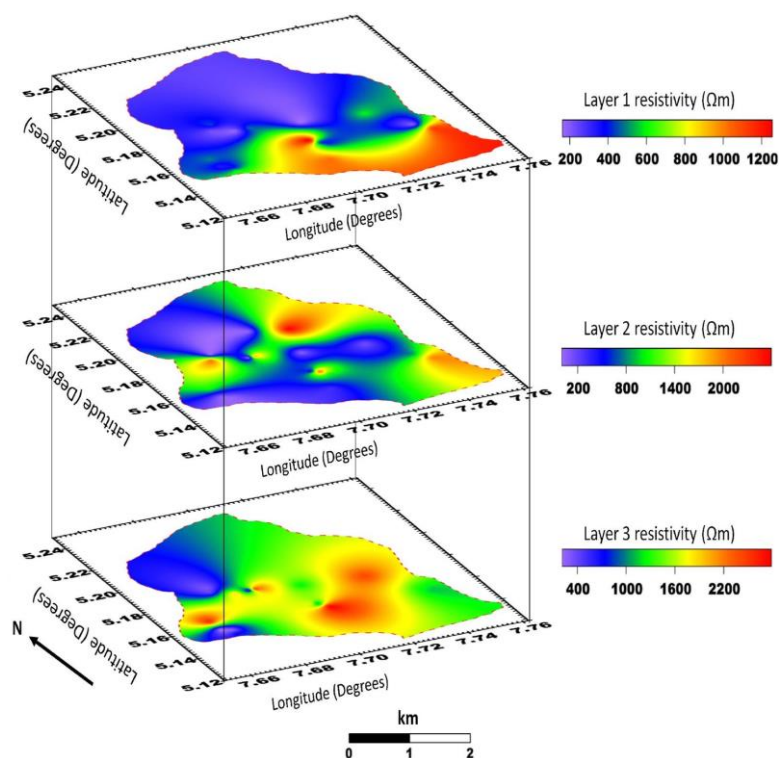

Fig. 9 Stacked image maps of layer 1, 2 and 3 resistivities. Layer 3 is the major exploitable aquifer in the study area.

The three layers in the southern half of the study region have rather high resistivity values, as depicted in *Fig. 9*. In certain areas of the research site, the final geoelectric layer had resistivity values ranging from 45.0 to 865.4 Ωm. In some sites (VESs 1, 4, 5, 8, 18, and 20), this layer was characterized as fine sand, whereas in other locations (VESs 11, 12, and 17), it was interpreted as sandy clay. The thickness and depth of the layer could not be established since the current did not reach the bottom of the layer at a maximum current electrode separation of 400 m in this study.

The ERT interpretation yields the electrical resistivity fluctuations of the near-surface layers. Two geoelectric layers were detected within the electrode spacing limit used, as indicated by the results given in *Fig. 7*. The resistivity values for the sample ERT stations depicted in *Fig. 7* exhibit an upward trend from the uppermost layer to the lower layers for ERTs 7 and 8, whereas the opposite is observed for ERTs 3 and 5. The results demonstrate a strong correlation with both the VES data and the borehole lithology information for the various locations, as depicted in *Fig. 7*.

3.2 | Results of Protectivity Assessment

This study utilized three secondary geoelectric indices to evaluate the level of protection provided by the hydrogeological units in the study area. The indices mentioned refer to the longitudinal conductance, resistivity reflection, and anisotropy coefficients of the aquifer protective layers (layers 1 and 2). These indices were calculated using the relevant equations provided in Section 3.3. *Table 2* provides a summary of the computed results. The longitudinal conductance varies between 0.02 and 0.85 Ω^{-1}, whereas the resistivity RC ranges from -0.84 to 0.85.

Additionally, the anisotropy coefficient extends from 1.00 to 1.48. The thickness of the aquifer overburden varies between 9.0 and 86.6 meters. *Fig. 10* displays the spatial arrangement of these factors within the

designated study region. Based on the combination of these factors, the image map of *Fig. 11* indicated four classes of protectivity.

Table 2. Results of the assessment of hydrogeological units' protectivity.

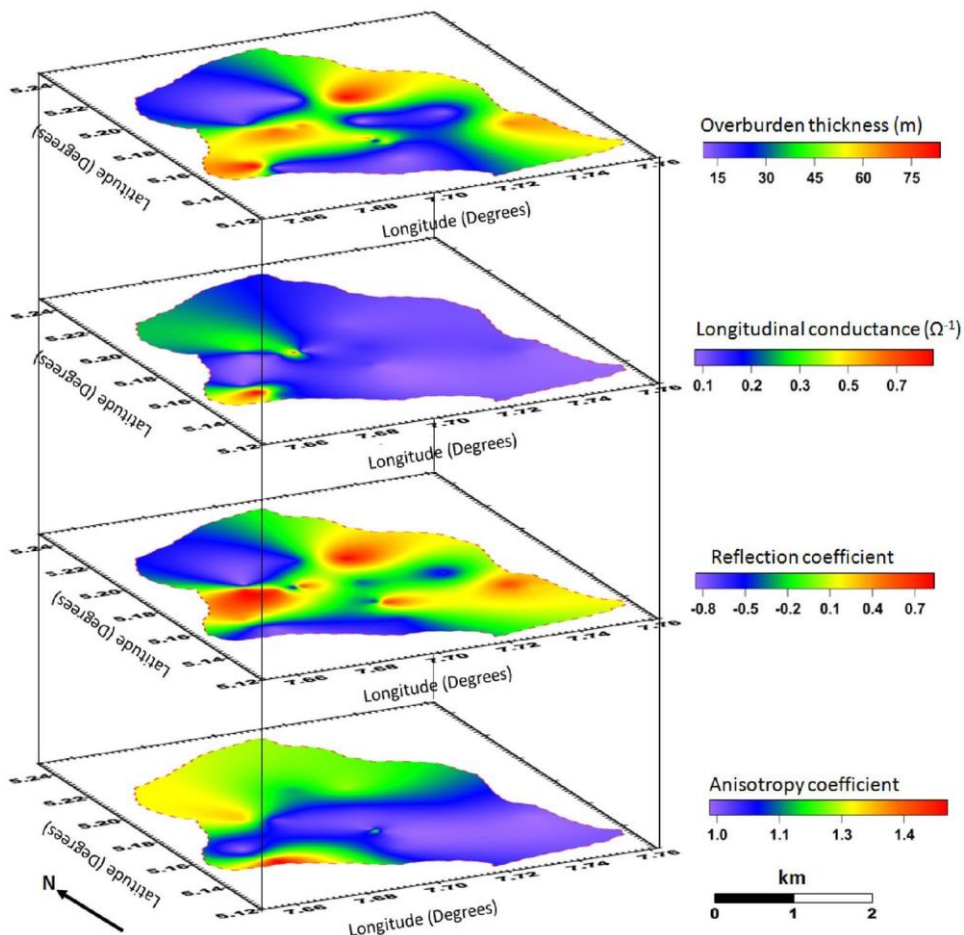| VES no	Location	Protecting Layers	Protecting Layer Resistivity (Ωm)	Thickness (m)	Longitudinal Conductivity S (Ω−1)	Resistivity RC	Anisotropy Coefficient	Aquifer Protectivity Rating
1	Dumpsite 1-utu ikpe	1	1190.2	2.6	0.04	− 0.65	1.24	Poor
		2	248.6	8.5				
2	Dumpsite 2-utu ikpe	1	1278.2	5.6	0.09	− 0.33	1.02	Poor
		2	639.4	56.7				
3	Utu ikpe near the prison	1	430.7	1.1	0.03	0.68	1.03	Poor
		2	2283.3	60.4				
4	Utu ikpe near palace	1	418.4	0.9	0.02	0.43	1.02	Poor
		2	1062.4	23.8				
5	Abiakpo edem idim	1	1028.8	0.6	0.03	− 0.50	1.03	Poor
		2	339.2	10.4				
6	Ibiakpan nto akan	1	193.5	1.6	0.09	0.62	1.03	Poor
		2	831.7	64.4				
7	Utu-uyo road	1	1131.8	2.1	0.03	0.28	1.00	Poor
		2	2004.7	61.0				
8	Ikpon road	1	590.7	1.3	0.08	− 0.60	1.10	Poor
		2	149.2	11.1				
9	Abiakpo ntak inyang	1	487.8	2.1	0.06	0.35	1.00	Poor
		2	1021.5	53.5				
10	Akwa poly 1	1	334.0	19.2	0.81	− 0.58	1.16	Good
		2	89.6	67.4				
11	Akwa poly 2	1	590.8	5.5	0.24	− 0.78	1.48	Moderate
		2	72.1	16.7				
12	Akwa poly 3	1	377.0	0.8	0.27	− 0.84	1.33	Moderate
		2	31.8	8.6				
13	Ikot ekpene housing, ifuho	1	441.5	3.6	0.04	0.61	1.06	Poor
		2	1848.3	63.4				
14	Ifuho	1	473.4	2.0	0.66	− 0.71	1.10	Moderate
		2	79.4	52.3				
15	Ifuho	1	170.7	1.7	0.08	0.69	1.04	Poor
		2	925.1	68.1				
16	Ibong ikot akan	1	228.5	6.1	0.05	0.80	1.31	Poor
		2	2111.6	49.3				
17	Ibong road	1	431.9	1.4	0.36	− 0.83	1.30	Moderate
		2	40.6	14.6				
18	Umuahia road	1	224.4	2.1	0.15	− 0.58	1.15	Weak
		2	59.1	8.4				
19	Ikono road	1	207.4	4.5	0.05	0.85	1.24	Poor
		2	2648.1	80.9				
20	Progress road	1	157.3	1.4	0.12	− 0.40	1.05	Weak
		2	66.8	7.6				
	Maximum				0.81	0.85	1.48	
	Minimum				0.02	− 0.84	1.00	

Fig. 10. Stacked image maps of overburden thickness, longitudinal conductivity, RC and anisotropy coefficient for assessing the aquifer protectivity in the study area.
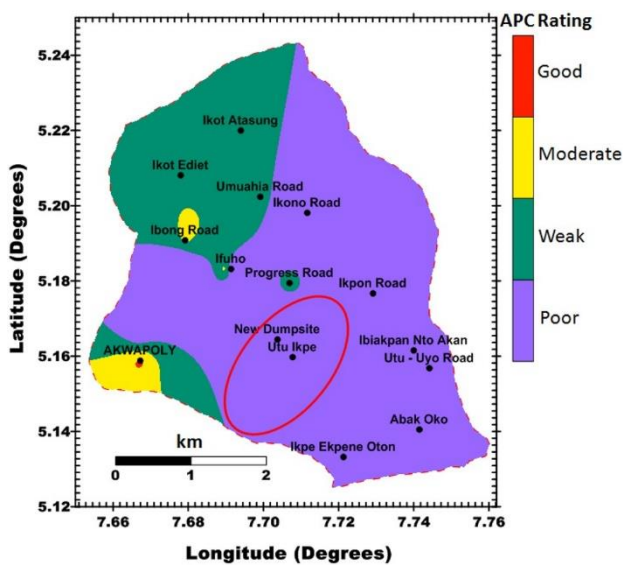

Fig. 11. Map showing the distribution of aquifer protectivity rating in the study area. The area on the map highlighted in red colour is the ravine where rainwater flows into the area.

The classes are presented in *Table 3* and align with the classifications of [11], [12] and the ratings of weak, moderate, and good protectivity.

Table 3. Aquifer protectivity rating based on longitudinal conductance.

S (Ω⁻¹)	Protectivity Rating
> 0.8	Good
0.24–0.66	Moderate
0.10–0.15	Weak
0.02–0.08	Poor

According to Abiola et al. [13], out of the 20 subjects etc. *Fig. 11* and *Fig. 12* depict the VES stations that were utilized in the study area. *Fig. 11* reveals that the hydrogeological units in the study area exhibit a low level of protectivity. Specifically, out of the 20 stations analyzed, 13 stations (65%) were rated as having poor protectivity, two stations (10%) were rated as having weak protectivity, and four stations (20%) were rated as having moderate protectivity. Only one station (5%) received a good protectivity rating. The distribution map in *Fig. 11* shows that the aquifers in the northeastern, central, and southeastern parts of the study area have a low level of protection. The remaining areas have a moderate level of protection, except for AKWAPOLY in the southwestern part of the area (VES 10), which has a high level of protection.
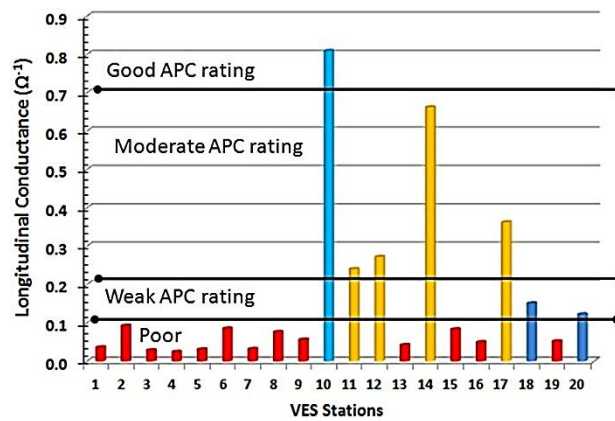
Fig. 12 Bar chart showing the aquifer protectivity rating of the VES stations in the study area.

The presence of a thick layer of impermeable protective material above the aquifer greatly increases its ability to prevent contamination from reaching the groundwater [4], [13]. Nevertheless, the southern-eastern portion of the study region (namely VES 2, 3, 4, 6, 9) exhibits zones with a substantial thickness of overburden composed of permeable fine/coarse sands. As a result, these layers do not have the capacity to effectively reduce the speed and filter the movement of fluids into the aquifer system, leading to a low protectivity rating. RC values below zero indicate the presence of a second layer composed of impermeable materials with low resistivity, whereas positive RC values suggest the presence of a second layer made up of permeable materials with high resistivity. Similarly, a negative RC indicates a moderate-to-good level of protection, whereas positive values indicate a poor-to-weak level of protection. Resistivity anisotropy occurs when the vertical resistivity is higher than the horizontal resistivity, indicated by an anisotropy coefficient λ greater than 1. When the resistivities in both directions are equal, the value of λ is 1, indicating isotropy. Specifically, resistivity remains constant regardless of the direction. Resistivity anisotropy can occur when there are alternating layers of thin-bedded sand and clay. Clay exhibits a high level of porosity and a low level of permeability, which means that it does not allow fluid to penetrate the subsurface easily. Based on the information provided, areas with negative RC values and an anisotropy coefficient larger than 1 indicate a moderate-to-good level of protectivity, as shown in *Fig. 10*. Nevertheless, the determining factor is the thickness of the overburden, which clarifies why the aquifer units are classified as having poor to weak protective qualities in specific areas (VES 1, 2, 5, 8, 18, and 20) while having negative RC and seeing anisotropy.

Both VES and ERT modelling results show that the uppermost layer, known as motley topsoil, is typically porous and permeable, with a resistivity range of 157.3–1278.2 Ωm. Typically, utility pipes for water distribution are buried within this layer. The pipes may experience corrosion if the resistivity of the topsoil is not sufficient. Resistivity levels below 10 Ωm are typically linked to highly corrosive layers. Levels ranging from 60 to 180 Ωm are connected with mildly corrosive layers, while values over 180 Ωm indicate non-

corrosive layers [41–43]. According to this categorization, the motley topsoil is generally not corrosive, except at VES 15 (with a resistivity of 170.7 Ωm) and VES 20 (with a resistivity of 157.3 Ωm), where the layer is somewhat corrosive. Therefore, utility pipes can be safely buried in the diverse topsoil in the research region without any concern for corrosion-related damage.

Fig. 9 illustrates the contrast between the flow directions of surface water (rainwater) and groundwater. Water moves from areas of higher elevation to areas of lower elevation, as described by Mc-Neill [44]. The surface topography map (topmost image map in *Fig. 13*) indicates that the northern portion of the study region has a higher elevation compared to the rest. This is consistent with the aquifer protectivity rating map shown in *Fig. 11*, where the ravine area is marked in red and has a low protectivity rating. The water table topography map (bottom image map in *Fig. 13*) shows a sink in the middle part, with pockets of elevated topography in the southeastern, northeastern, and western regions of the research area. Groundwater predominantly migrates towards the central region, aligning with the direction of surface water flow into the ravine. The direction of groundwater flow is significant since it coincides with the direction of any subsurface pollutant movement in the vicinity. Upon careful analysis of *Fig. 13*, it becomes apparent that the water table closely resembles the surface topography, albeit in a less pronounced manner. Consequently, any underground pollution plumes will migrate towards the central region of the research area.
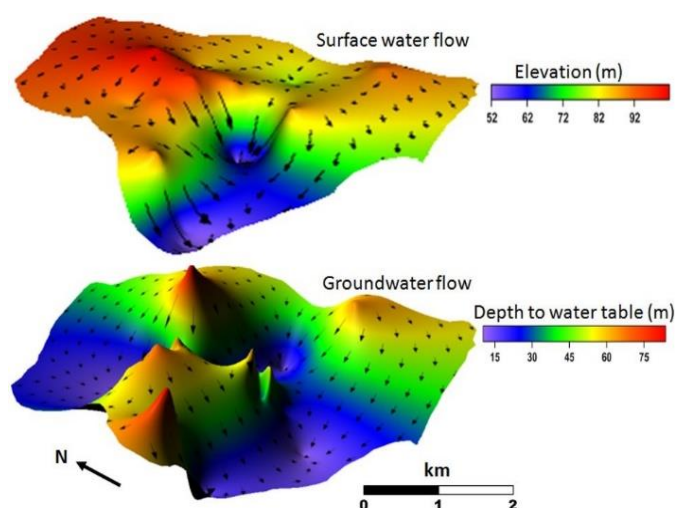

Fig. 13. Stack map of surface and water table topography showing the directions of surface and groundwater flows.

3.3 | Conclusion

This study utilized the geoelectric method, specifically the VES and ERT techniques, to evaluate the protective capacity of hydrogeological units in the area of Ikot Ekpene Urban and its surrounding regions in Southern Nigeria. The VES data were manually interpreted using the partial curve matching technique and quantitatively analyzed using the WINRESIST computer software program. The ERT data were interpreted using the RES2DINV computer software tool. The VES data indicate that the studied area consists of 3–4 geoelectric layers. The predominant composition of these layers consists of sandy materials, including fine, coarse, and gravelly particles. However, in certain areas, there are clay intercalations, as shown by the borehole lithological data that is currently available. The primary hydrogeological formations are found in the third layer, exhibiting resistivity values ranging from 214.4 to 2839.0 Ωm. The thickness of the layers that protect the overburden ranges from 9.0 to 86.6 m. The protectivity of the hydrogeological units in the area was assessed using the longitudinal conductance, resistivity RC, and anisotropy coefficient of the protecting layers. The study region has been categorized into four zones based on the distribution of these secondary geoelectric indices, with each zone assigned a protectivity grade. Out of the aquifer units in the area, 65% have a poor protectivity rating, 10% have a weak rating, 20% have a moderate rating, and 5% have an excellent rating. The water table appears to be a less intense version of the surface topography, indicating that any underground

contamination plumes will move towards the central region of the study area. The ERT image sections depict the fluctuations in resistivity at a shallow depth and exhibit a strong correlation with the VES results.

References

[1] Reilly, T. E., Dennehy, K. F., Alley, W. M., & Cunningham, W. L. (2008). *Ground-water availability in the united states*. US Geological Survey Circular. https://doi.org/10.3133/cir1323

[2] George, N. J., Ibanga, J. I., & Ubom, A. I. (2015). Geoelectrohydrogeological indices of evidence of ingress of saline water into freshwater in parts of coastal aquifers of Ikot Abasi, southern Nigeria. *Journal of african earth sciences*, *109*, 37–46. DOI: 10.1016/j.jafrearsci.2015.05.001

[3] Thomas, J. E., George, N. J., Ekanem, A. M., & Nsikak, E. E. (2020). Electrostratigraphy and hydrogeochemistry of hyporheic zone and water-bearing caches in the littoral shorefront of Akwa Ibom State University, Southern Nigeria. *Environmental monitoring and assessment*, *192*(8), 1–19. DOI: 10.1007/s10661-020-08436-6

[4] Bayewu, O. O., Oloruntola, M. O., Mosuro, G. O., Laniyan, T. A., Ariyo, S. O., & Fatoba, J. O. (2018). Assessment of groundwater prospect and aquifer protective capacity using resistivity method in Olabisi Onabanjo University campus, Ago-Iwoye, Southwestern Nigeria. *NRIAG journal of astronomy and geophysics*, *7*(2), 347–360. DOI: 10.1016/j.nrjag.2018.05.002

[5] Umar, N. D., & Igwe, O. (2019). Geo-electric method applied to groundwater protection of a granular sandstone aquifer. *Applied water science*, *9*(4), 1–14. DOI: 10.1007/s13201-019-0980-2

[6] Esu, E. O., & Amah, E. A. (1999). Physicochemical and bacteriological quality of natural waters in parts of Akwa Ibom and Cross River States, Nigeria Global J. *Pure and applied science*, *5*(4), 525–534.

[7] Uchegbu, S. N. (2002). *Issues and strategies in environmental planning and management in nigeria.enugu-nigeria*. Spotlite publishers.

[8] Oseji, J. O., Egbai, J. C., Okolie, E. C., & Ese, E. C. (2018). Investigation of the aquifer protective capacity and groundwater quality around some open dumpsites in sapele delta state, Nigeria. *Applied and environmental soil science*, *2018*(1), 3653021. DOI: 10.1155/2018/3653021

[9] Olorunfemi, M. O., Ojo, J. S., & Akintunde, O. M. (1999). Hydro-geophysical evaluation of the groundwater potentials of the Akure Metropolis, Southwestern Nigeria. *Journal of mining and geology*, *35*(2), 207–228.

[10] Adeniji, A. E., Omonona, O. V., Obiora, D. N., & Chukudebelu, J. U. (2014). Evaluation of soil corrosivity and aquifer protective capacity using geoelectrical investigation in Bwari basement complex area, Abuja. *Journal of earth system science*, *123*(3), 491–502. DOI: 10.1007/s12040-014-0416-1

[11] Henriet, J. P. (1976). Direct Applications of the dar zarrouk parameters in ground water surveys. *Geophysical prospecting*, *24*(2), 344–353. DOI: 10.1111/j.1365-2478.1976.tb00931.x

[12] Oladapo, M., & Akintorinwa, O. (2007). Hydrogeophysical study of Ogbese South Western Nigeria. *Global journal of pure and applied sciences*, *13*(1), 55–61. DOI: 10.4314/gjpas.v13i1.16669

[13] Abiola, O., Enikanselu, P. A., & Oladapo, M. I. (2009). Groundwater potential and aquifer protective capacity of overburden units in Ado-Ekiti, southwestern Nigeria. *International journal of physical sciences*, *4*(3), 120–132.

[14] Mogaji, K. A., Omosuyi, G. O., & Olayanju, G. M. (2011). Groundwater system evaluation and protective capacity of overburden material at Ile-olujI, Southwestern Nigeria. *Journal of geology and mining research*, *3*(11), 294–304. http://www.academicjournals.org/JGMR

[15] Ekanem, A. M. (2020). Georesistivity modelling and appraisal of soil water retention capacity in Akwa Ibom State University main campus and its environs, Southern Nigeria. *Modeling earth systems and environment*, *6*(4), 2597–2608. DOI: 10.1007/s40808-020-00850-6

[16] Ekanem, A. M., George, N. J., Thomas, J. E., & Nathaniel, E. U. (2020). Empirical relations between Aquifer geohydraulic–geoelectric properties derived from surficial resistivity measurements in parts of akwa ibom state, Southern Nigeria. *Natural resources research*, *29*(4), 2635–2646. DOI: 10.1007/s11053-019-09606-1

[17] Ekanem, A. M., Akpan, A. E., George, N. J., & Thomas, J. E. (2021). Appraisal of protectivity and corrosivity of surficial hydrogeological units via geo-sounding measurements. *Environmental monitoring and assessment*, *193*(11), 1–22. DOI: 10.1007/s10661-021-09518-9

[18] Ayuk, M. A. (2020). Groundwater aquifer vulnerability assessment using a dar-zarrouk parameter in a proposed aboru residential estate, Lagos State, Nigeria. *Journal of applied sciences and environmental management*, *23*(12), 2081. DOI: 10.4314/jasem.v23i12.2

[19] Yeboah-Forson, A., & Whitman, D. (2014). Electrical resistivity characterization of anisotropy in the Biscayne Aquifer. *Groundwater*, *52*(5), 728–736. DOI: 10.1111/gwat.12107

[20] Bała, M., & Cichy, A. (2015). Evaluating electrical anisotropy parameters in miocene formations in the cierpisz deposit. *Acta geophysica*, *63*(5), 1296–1315. DOI: 10.2478/s11600-014-0252-3

[21] Umoh, S. D., & Etim, E. E. (2013). Determination of heavy metal contents from dumpsites within. *The international journal of engineering and science*, *2*(2), 123–129.

[22] George, N. J., Ubom, A. I., & Ibanga, J. I. (2014). Erratum: Integrated approach to investigate the effect of leachate on groundwater around the Ikot ekpene dumpsite in Akwa Ibom state, Southeastern Nigeria. *International journal of geophysics*, *2014*. DOI: 10.1155/2014/636129

[23] Mbipom, E. W., Okwueze, E. E., & Onwuegbuche, A. A. (1996). Estimation of transmissivity using VES data from the Mbaise area of Nigeria. *Nigerian journal of physics*, *85*, 28–32.

[24] K. C. Short, A. J. S. (1967). Outline of geology of Niger Delta. *AAPG bulletin*, *51*(5), 761–779. DOI: 10.1306/5d25c0cf-16c1-11d7-8645000102c1865d

[25] Stacher, P. (1995). Present understanding of the Niger Delta hydrocarbon habitat. In *Geology of deltas* (pp. 257–267). Taylor & Francis.

[26] Reijers, T. J. A., & Petters, S. W. (1987). Depositional environments and Diagenesis of Albian Carbonates on the Calabar Flank, Se Nigeria. *Journal of petroleum geology*, *10*(3), 283–294. DOI: 10.1111/j.1747-5457.1987.tb00947.x

[27] Esu, E. O., Okereke, C. S., & Edet, A. E. (1999). A regional hydrostratigraphic study of Akwa Ibom State, southeastern Nigeria. *Global journal of pure and applied sciences*, *5*, 89–96.

[28] Edet, A. E., & Okereke, C. S. (2002). Delineation of shallow groundwater aquifers in coastal plain sands of Calabar area (Southern Nigeria) using surface resistivity and hydrogeological data. *Journal of african earth sciences*, *35*(3), 433–443. DOI: 10.1016/S0899-5362(02)00148-3

[1] [29]   Asaah, A. V. (2011). *Geology and mineral resources of nigeria*. Economic Geology. Springer. https://doi.org/10.2113/econgeo.106.3.523

[30] Ward, S. H. (1987). Electrical methods in geophysical prospecting. *Methods in experimental physics*, *24*, 265–375. DOI: 10.1016/S0076-695X(08)60601-8

[31] Dobrin, M. B. (1981). *Introduction to geophysical prospecting*. , 4 Introduction to geophysical prospecting. 3rd edition. (Vol. 4). McGraw-hill New York.

[32] Zohdy, a. a. R., Eaton, G. P., & Mabey, D. R. (1974). Application of surface geophysics to ground-water investigations. *Techniques of water-resources investigations of the united states geological survey*, 123. DOI: 10.3133/twri02D1

[33] Vander Velpen, B. P. A., & Sporry, R. J. (1993). RESIST. A computer program to process resistivity sounding data on pc compatibles. *Computers and geosciences*, *19*(5), 691–703. DOI: 10.1016/0098-3004(93)90102-B

[34] Bandani, E., & Moghadam, M. A. (2011). Application of groundwater mathematical model for assessing the effects of galoogah dam on the shooro aquifer- Iran. *European journal of scientific research*, *54*(4), 499–511.

[35] Loke, M. H., & Barker, R. D. (1996). Rapid least-squares inversion of apparent resistivity pseudosections by a quasi-Newton method. *Geophysical prospecting*, *44*(1), 131–152. DOI: 10.1111/j.1365-2478.1996.tb00142.x

[36] Loke, M. H., & Dahlin, T. (2002). A comparison of the Gauss-Newton and quasi-Newton methods in resistivity imaging inversion. *Journal of applied geophysics*, *49*(3), 149–162. DOI: 10.1016/S0926-9851(01)00106-9

[37] Loke, M. H., Acworth, I., & Dahlin, T. (2003). A comparison of smooth and blocky inversion methods in 2D electrical imaging surveys. *Exploration geophysics*, *34*(3), 182–187. DOI: 10.1071/EG03182

[38] Bello, A. M. A., Makinde, V., & Coker, J. O. (2010). Geostatistical analyses of accuracies of geologic sections derived from interpreted vertical electrical soundings (VES) data: an examination based on VES and Borehole data collected from the Northern Part of Kwara State, Nigeria. *Journal of american science*, *6*(2), 24–31.

[39] Chemali, R., Gianzero, S., & Su, S. M. (1987). The effect of shale anisotropy on focused resistivity devices. *SPWLA 28th annual logging symposium*. SPWLA. https://www.onepetro.org/

[40] George, N. J., Obianwu, V. I., Akpan, A. E., & Obot, I. B. (2010). Assessment of shallow aquiferous units and their coefficients of anisotropy in the coastal plain sands of Southern Ukanafun local government area, Akwa Ibom State, Southern Nigeria. *Indian archives of physics res*, *1*(2), 118–128.

[41] Agunloye, O. (1984). Soil aggressivity along steel pipeline route at Ajaokuta southwestern Nigeria. *Journal of mining and geology*, *21*, 97–101.

[42] Oladapo, M. I., Mohammed, M. Z., Adeoye, O. O., & Adetola, B. A. (2004). Geoelectrical investigation of the Ondo State Housing Corporation Estate Ijapo Akure, southwestern Nigeria. *Journal of mining and geology*, *40*(1), 41–48. DOI: 10.4314/jmg.v40i1.18807

[43] Mosuro, G. O., Omosanya, K. O., Bayewu, O. O., Oloruntola, M. O., Laniyan, T. A., Atobi, O., … Adekoya, F. (2017). Assessment of groundwater vulnerability to leachate infiltration using electrical resistivity method. *Applied water science*, *7*(5), 2195–2207. DOI: 10.1007/s13201-016-0393-4

[44] Mc-Nell, J. D. (1980). Electrical conductivity of soil and rocks. *Geonics limited*, *17*, 1197–1211. https://geonics.com/pdfs/technicalnotes/tn5.pdf